Rotational breakup as the origin of small binary asteroids

Kevin J. Walsh[1,2], Derek C. Richardson[2] and Patrick Michel[1]

[1]UMR 6202 Cassiopée, University of Nice-Sophia Antipolis, CNRS, Observatoire de la Côte d'Azur, B.P. 4229, 06304 Nice Cedex 4, France [2]Department of Astronomy, University of Maryland, College Park, Maryland, 20742-2421, USA

Asteroids with satellites are observed throughout the Solar System, from sub-km near-Earth asteroid (NEA) pairs, to large and distant systems in the Kuiper Belt. The smallest and closest systems are found among NEAs and small inner Main Belt asteroids (MBAs), typically have rapidly rotating primaries and close secondaries on circular orbits, and account for ~15% of NEAs and MBAs with diameters under 10 km[1,2]. The mechanism that forms such similar binaries in these two dynamically different populations was unclear until now. Here we show that these binaries are created by the slow spin up of a "rubble pile" asteroid via the thermal YORP effect. We find that mass shed from the equator of a critically spinning body accretes into a satellite if the material is collisionally dissipative and the primary maintains a low equatorial elongation. The satellite naturally forms mostly from material originating near the primary's surface and enters into a close, low-eccentricity orbit. The properties of binaries produced by our model match those currently observed in the small NEA and MBA populations, including 1999 KW_4[3,4].

The angular momentum content from the primary's rotation and the secondary's orbit among small binaries suggests the satellites were formed by rotational disruption after the body was pushed beyond its critical spin limit[2,5]. Tidal encounters can account for near-critical spin rates and are efficient at forming binaries from rubble piles, however they are even more efficient at subsequently dissociating those binaries due to repeated planetary encounters[6,7]. In the Main Belt, the catastrophic disruption of an asteroid can produce binary systems, but they do not match the observed properties of small binaries[8,9]. Radar observations of binary NEA 1999 KW_4 show that the primary is oblate with a pronounced equatorial belt, the effective gravity at the equator is directed inward, but is nearly zero, and its equatorial elongation is nearly unity[3,4]. Owing to the quality of the observations, and the diagnostic "top-like" shape of the primary, this system is a key constraint for binary formation models. The small Main Belt asteroid (SMBA) binaries have properties nearly identical to those of the NEA binaries and both have an estimated frequency of ~15%[2]. This suggests a common formation mechanism, which has not been identified so far.

One mechanism that operates on both NEAs and MBAs that may lead to the observed binaries is YORP-induced spinup, which arises from reflection and/or absorption and re-radiation of sunlight by the surface of an irregularly shaped asteroid[12,13]. This effect accounts for the rotation-rate increase of NEAs 2000 PH_5 and 1862 Apollo[14,15,16]. The timescale for YORP spin alteration depends on the size R of the body (increasing with R^2), the distance a from the Sun (increasing with a^2), the body's thermal properties, and the body's shape and obliquity. The YORP spinup/spindown timescale for kilometre-size NEAs and MBAs is estimated to be between a few 10^4 and 10^6 yrs depending on the shape and makeup of the asteroid[12,17]. Due to a notable abundance of both fast and slow rotators among NEAs and SMBAs, this effect appears to act widely[18]. However, it has never been demonstrated whether gradual spinup leads to mass loss that can form binaries, and if so, whether those binaries are a close match to observations.

We carried out numerical simulations of YORP spinup of a cohesionless body consisting of ~1000, self-gravitating, rigid spheres. Several lines of evidence suggest that most kilometre-size objects are rubble piles or gravitational aggregates, which means they lack cohesion but are non-fluid[19]. One indicator of such bodies' response to stress is the angle of friction (ϕ) of the material. We modelled different kinds of rubble piles, ranging from a fluid-like body (ϕ ~ 0°), to a more typical terrestrial material (ϕ ~ 40°, to be referred to as the *nominal case*)[20]. The model rubble piles consisted of either monodisperse spheres, or a simple bi-modal distribution (meaning two different sizes of particles). Numerical experiments show that monodisperse rubble piles behave similarly to a body with ϕ ~ 40°, whereas ϕ for bi-modal rubble piles depends on the relative particle sizes and their relative abundance within the body[20]. For our bi-modal models, ϕ ranged from near 0° to ~ 20°. We also tested another possible asteroid internal structure consisting of a rigid core of large particles surrounded by loose smaller particles. The representation of such a case by an angle of friction is not straightforward.

For the nominal case of ϕ ~ 40°, experiments were run using two different initial asteroid shapes: spherical and prolate. The prolate body had axis ratios of 2:1:1, and both shapes had initial spin periods of 4.4 h, longer than their stability limits for the body bulk density of 2.2 g cm^{-3} (where each particle had a density of 3.4 g cm^{-3}), so there was no immediate reshaping or collapsing. As the spin rate was increased (see Fig. 2) and approached the critical spin limit, the spherical bodies became oblate, with mass moving from the poles to the equator. After this initial global reshaping of the spherical body, an equatorial belt of material remained, and subsequent mass loss originated from this region (Figs. 1 and 2).

The fate of the ejected mass depends on the primary shape and the coefficient of restitution (the ratio of rebound to impact speed owing to energy dissipation when particles collide). In simulations with initially prolate bodies, the ejected mass does not readily accumulate into a satellite, because the mass that is ejected is lifted into a very shallow orbit barely above the surface of the primary and is easily disturbed by equatorial asymmetries in the prolate primary. In contrast, particles dislodged from spherical or oblate primaries quickly and efficiently accumulate into a satellite. For the most ideal parameters, $\phi \sim 40°$ and a very low coefficient of restitution, the satellites accrete over 90% of all ejected particles. In cases where the primary shape is not initially spherical or oblate, satellite accumulation is delayed until the primary achieves a favourable shape.

The tendency of a gravitational aggregate to adopt an oblate shape as the angular momentum is increased is contrary to the evolution of fluid shapes (the classical Jacobi and MacLaurin figures), which become approximately prolate at rapid rotation rates. Simulations with $\phi \sim 20°$ or 0° behaved most like the classical fluid case. The cases with $\phi \sim 0°$ immediately adopted elongated shapes and maintained prolate shapes during mass loss, frustrating satellite formation for all test parameters. The intermediate test case, with $\phi \sim 20°$, represented a transition, where binary formation was possible but not very efficient. In our other test case of a substantial rigid core surrounded by smaller, loose particles, the core limited the overall elongation caused by motions of surface material arising from rapid rotation. Thus, a low equatorial elongation was maintained, permitting satellite formation (Fig. 3). Essentially, the minimum requirement for satellite formation is a low equatorial elongation, which was achieved in our models for aggregates with large non-zero angle of friction (which restricts reshaping), or aggregates with a substantial rigid core. In fact, Itokawa, the first asteroid in this size range to be visited by spacecraft, has a morphology suggestive of a large core surrounded by smaller debris[21].

For our nominal case, massive satellites of minimum radius 0.2 $R_{\rm pri}$ formed in all simulations for which the lowest tested value of coefficient of restitution was used (0.2, where 1 is perfectly elastic and 0 is completely dissipative). Efficiency of satellite formation declined as the coefficient of restitution was increased, until, above a value of 0.6, no satellites formed. Evidently satellite accumulation is sensitive to energy dissipation during collisions, suggesting that collisions on the order of ~0.2–0.5 m s^{-1} between asteroidal material dissipate significant amounts of energy. The actual value of the coefficient of restitution during collisions is not well constrained experimentally, but small-scale experiments suggest that it depends on the impact speed and material properties[22,23]. Values as low as 0.2 can be expected, in particular for bodies with a certain degree of porosity[22], such as low-density asteroids and asteroids belonging to dark taxonomic type. Moreover, since the YORP timescale is inversely proportional to density, this model of binary formation is favoured for bodies with low bulk densities, or those consisting of collisionally dissipative materials. However, the YORP timescales are very short compared to dynamical lifetimes, so this mechanism may be indistinguishable between taxonomies. Currently all major taxonomic types are found amongst the observed binary systems, with no identifiable trends yet.

The exact properties of the secondary and its orbit depend strongly on when the YORP effect ceases to increase the spin of the primary and send mass to the secondary[20]. In our simulations, when secondaries grow to 0.3 R_{pri}, the orbital semi-major axes are between 2–4.5 R_{pri}, eccentricities are all below 0.15, and the equatorial elongations of the primaries are all below 1.2. Most (70–90%) of the particles comprising the secondary originate from the surface of the primary. After the secondary forms, 15–35% of the primary's surface is material that originated below the surface and is exposed mostly near the poles of the primary, while the equator is still largely covered with original surface material (see Fig. 1). The near absence of observed binary systems with very large secondaries, larger than about half the size of the primary, suggests that mass transfer stops at some point. Our simulations only model the gradual spinup of a single asteroid, and not the additional complex effects a large secondary in a close orbit may produce, such as the binary YORP effect (BYORP, a radiation effect operating on the system rather than the primary only), tidal interactions, or continued reshaping of the primary. Therefore the long-term fate of the system depends on the evolution of the binary, with the BYORP effect or planetary tides possibly splitting the system, leaving behind a rapidly rotating primary[20].

The observed NEA and SMBA binary fraction (~15%) is likely a balance between YORP spinup and known or suspected dynamical sinks (planetary tides and BYORP). The similarities between binaries in the dynamically distinct NEA and SMBA populations arise from their shared minimum physical requirements for binary formation via YORP, properties that must be found among a larger population of asteroids that participate in the binary formation/destruction cycle. The requirements include a non-zero angle of friction for the component material (or a rigid core that resists re-shaping under stress from rapid rotation), allowing oblate/spherical shapes to be maintained near the critical spin limit, and subsequently permitting stable satellite formation (which itself is dependent on a certain degree of collisional dissipation in the component material). These systems may be particularly attractive targets for space missions, due to the exposure of some fresh surface by the movement and removal of surface material from the poles to equator of the asteroid.

1. Pravec, P. *et al*. Photometric survey of binary near-Earth asteroids. *Icarus*, **181**, 63-93 (2006).

2. Pravec, P., and Harris, A.W. Binary Asteroid Population. *Icarus*, **190**, 250-259 (2007).

3. Ostro, S. J. *et al.* Radar Imaging of Binary Near-Earth Asteroid (66391) 1999 KW4. *Science*, **314**, 1276-1280 (2006).

4. Scheeres, D. *et al.* Dynamical Configuration of Binary Near-Earth Asteroid (66391) 1999 KW4. *Science*. **314**. 1280-1283 (2006).

5. Richardson, D. C. & Walsh, K. J. Binary Minor Planets. *Annual Review of Earth and Planetary Sciences*, **34**, 47-81 (2006).

6. Walsh, K. J. & Richardson, D. C. Binary near-Earth asteroid formation: Rubble pile model of tidal disruptions. *Icarus.* **180**, 201-216 (2006).

7. Walsh, K. J. & Richardson, D. C. A steady-state model of NEA binaries formed by tidal disruption of gravitational aggregates. *Icarus.* **193**, 553-566 (2008).

8. Michel, P., *et al*. Collisions and gravitational reaccumulation: forming asteroid families and satellites. *Science*, **294**, 1696-1700 (2001).

9. Durda, D. D. *et al*. The formation of asteroid satellites in catastrophic impacts:

Results from numerical simulations. *Icarus* **167**, 382–396 (2004).

11. Margot, J. L. *et al.* Binary Asteroids in the Near-Earth Object Population. *Science*, **296**, 1445-1448 (2002).

12. Rubincam, D. P. Radiative spin-up and spin-down of small asteroids. *Icarus*, **148**, 2-11 (2000).

13. Paddack, S.J. & Rhee, J.W. Rotational bursting of interplanetary dust particles. *Geophysical Research Letter* **2**, 365-367 (1975).

14. Lowry, S.C., *et al*. Direct detection of the YORP effect. *Science*, **316**, 272-274 (2007).

15. Taylor, P, A., *et al.* Spin Rate of Asteroid (54509) 2000 PH5 Increasing Due to the YORP Effect. *Science.* **316**, 274-277 (2007).

16. Kaasalainen, M, Ďurech, J., Warner, B. D., Kugly, Y. N., Gaftonyuk, N. N., Acceleration of the rotation of asteroid 1862 Apollo by radiation torques. *Nature.* **446**, 420-422 (2007).

17. Ćuk, M. Formation and Destruction of Small Binary Asteroids. *The Astrophysical Journal*. **659**, 57-60 (2007).

18. Pravec, P., & Harris, A. W., Fast and Slow Rotation of Asteroids. *Icarus*. **148**, 12-20 (2000).

19. Richardson, D. C., Leinhardt, Z. M., Melosh, H. J., Bottke, W. F., & Asphaug, E. . in *Asteroids III* (eds. W. F. Bottke Jr., A. Cellino, P. Paolicchi, and R. P. Binzel.) Gravitational Aggregates: Evidence and Evolution. 501-515 (2002).

20. Richardson, D. C., Elankumaran, R. E., & Sanderson, R. E., Numerical experiments with rubble piles: equilibrium shapes and spins. *Icarus.* **173**, 349-361 (2005).

21. Fujiwara *et al*. The rubble-pile asteroid Itokawa as observed by Hayabusa. *Science* **312**, 1330-1334 (2006).

22. Supulver, K. D., Bridges, F. G., & Lin, D. N. C., The coefficient of restitution of ice particles in glancing collisions: Experimental results for unfrosted surfaces. *Icarus*. **113**, 188-199 (1995).

23. Fujii, Y., and Nakamura, A.M. Compaction and fragmentation of porous targets at low velocity collisions. LPSC XXXVIII, 1525 (2007).

KJW and DCR acknowledge support from the National Science Foundation under grants AST0307549 and AST0708110. KJW and PM also had the support of the ESA's Advanced Concepts Team on the basis of the Ariadna study 07/4111 "Asteroid Centrifugal Fragmentation," and of the French Programme National de Planétologie. KW is also supported by the Henri Poincaré fellowship at the Observatoire de la Côte d'Azur, Nice, France. We acknowledge the use of the Mésocentre de Calcul-SIGAMM hosted at the Observatoire de la Côte d'Azur, Nice, France. Some simulations were carried out at the University of Maryland using the Department of Astronomy `borg` cluster and the Office of Information Technology High Performance Computing Cluster. Raytracing for Figs. 1 and 3 was performed using the Persistence of Vision Raytracer. We are grateful to Bill Bottke and Alan Harris for their constructive reviews.

Correspondence and requests for materials should be addressed to K.W. (kwalsh@oca.eu).

Figure 1. **Asteroid shape change during mass-loss.** The snapshots show the gradual change in shape that an initially prolate (top) and spherical (middle) body undergoes, as seen looking in the plane of the asteroid's equator. Also shown (bottom) is the movement and loss of a body's original surface particles (orange) and the exposure of the interior particles (white) during the binary formation. The top two panels show only the largest body in the simulation; ejected mass is not shown. Material that accumulates into a satellite does so slowly and from material lost from the equator of the primary; there is no large-scale "fission" event. The time between images is roughly 1000 asteroid rotations for the top two panels, though the simulations are sped up compared to the actual YORP effect for computational efficiency. Prolate bodies become less elongated as particles are ejected from the ends of the long axis, reducing the critical rate for mass loss. Eventually prolate bodies become oblate, ending up with similar axis ratios as for the case of an initially spherical body.

Figure 2. **Primary and secondary properties during satellite formation.** Evolution of (a) primary spin rate, (b) primary axis ratios (dark: intermediate to long axis; grey: short to long axis), (c) mass loss (solid line) and satellite size (grey dashed line) as a percentage of progenitor mass, (d) and satellite eccentricity, as a function of ~50 sec-interval timesteps. The originally spherical body becomes oblate after the increasing spin rate causes some mass loss. The newly oblate primary begins to accumulate mass in one satellite (dashed line in plot c), and the eccentricity quickly drops to very low values. Initially prolate bodies show similar mass loss, but do not accrete a satellite until becoming oblate. The slow YORP spinup is modelled by applying small, discrete increases to the angular momentum of each particle making up the body, relative to the body center of mass. If any mass has been ejected or is in orbit, it is exempt from the angular momentum addition. The spin boosts are applied approximately every 5 rotation periods (for periods ~ 3 h), allowing time for the body to equilibrate before more angular momentum is added to the system. If there is mass lost between spin boosts, the next spin boost is delayed for at least ~10 rotations, though these results were unchanged over a wide range of delay times between spin boosts.

Figure 3. **Binary formation for an asteroid with a rigid core.** Snapshot of binary formation for a body with a core of organised large particles (grey), making up ~30% of the total mass, surrounded by smaller particles (white). Shown are two views of the system at the same point in time: looking down the primary spin axis (left—only the primary is shown), and looking along the plane of the primary's equator and secondary's orbit (right). The core minimizes equatorial elongation growth, allowing satellite formation. In tests with a smaller core the body becomes very elongated and satellite formation is entirely frustrated.

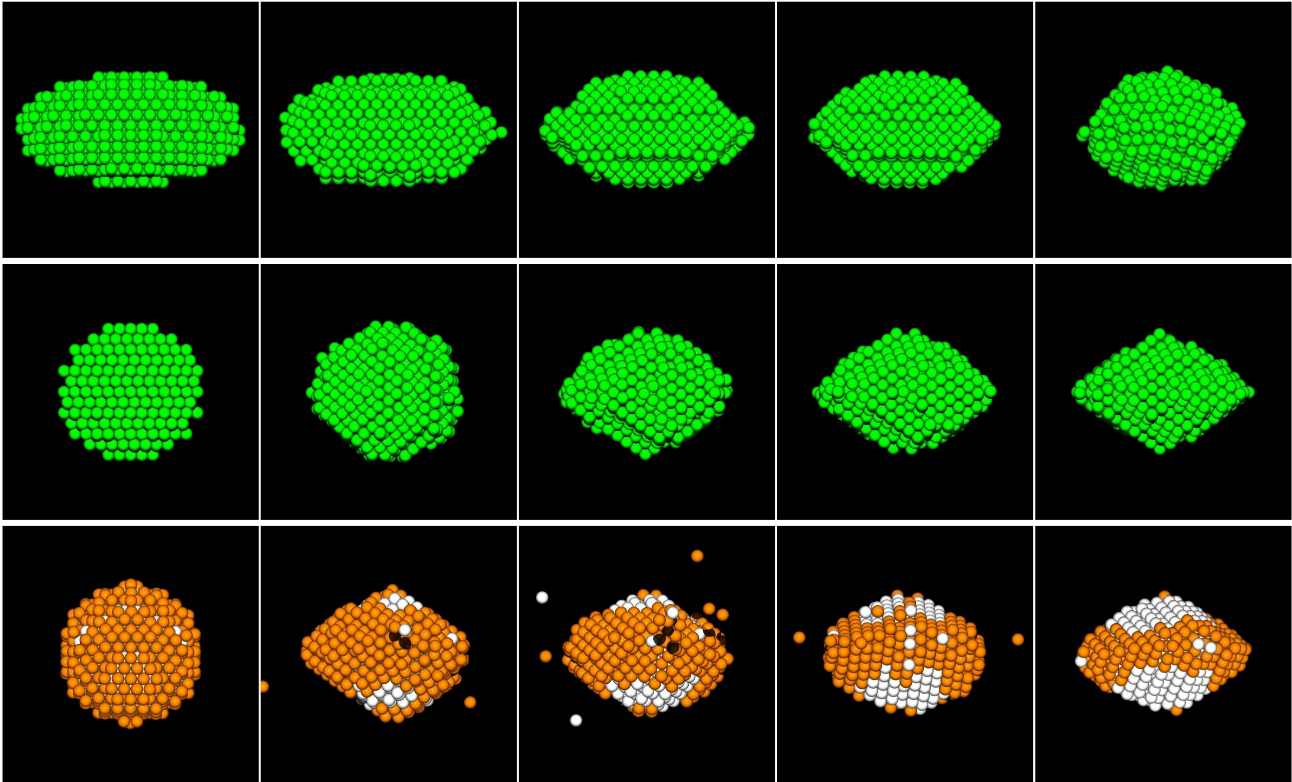

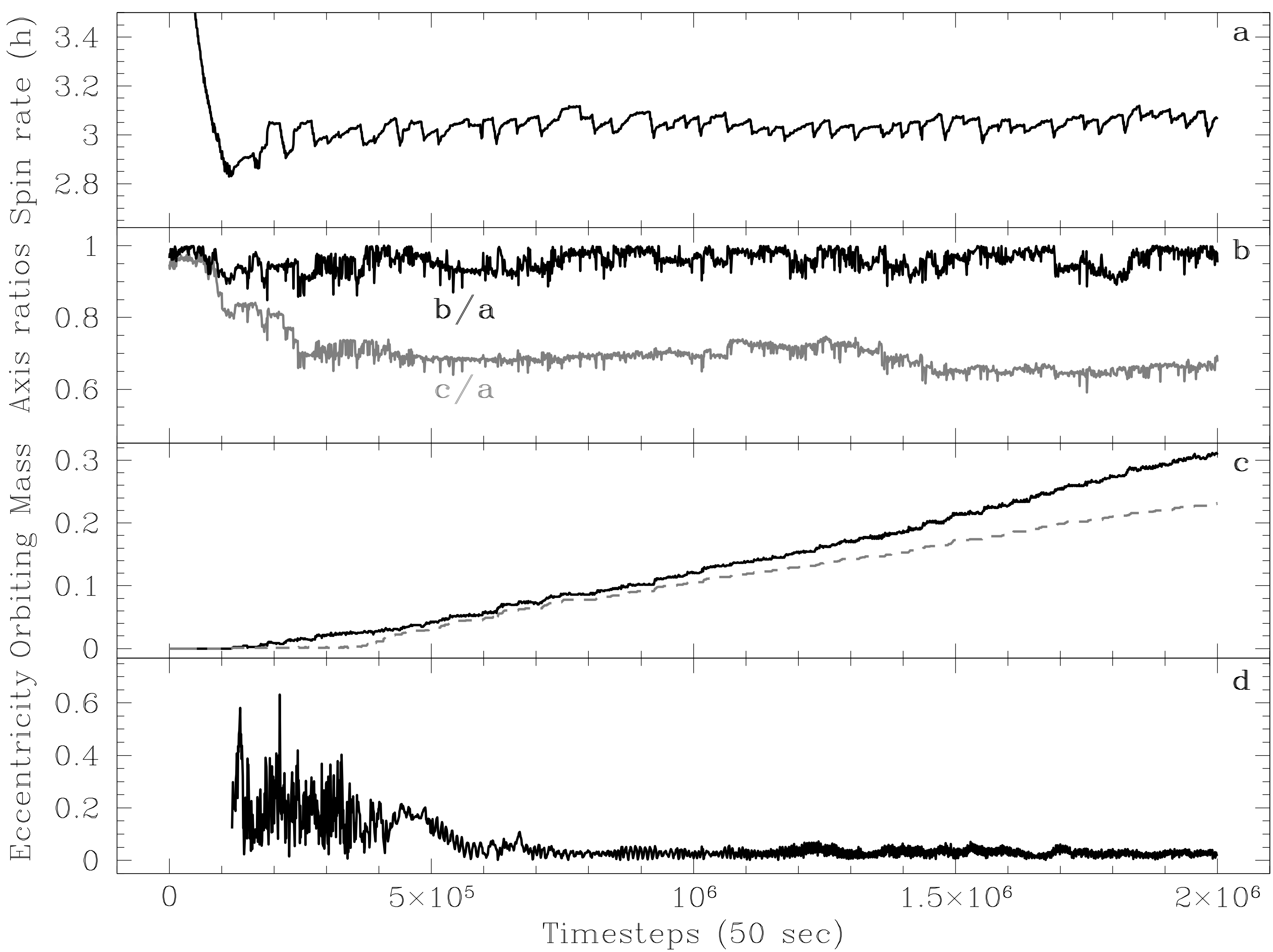
Spin rate (h)
3.4
3.2
3
2.8
a
Axis ratios
1
0.8
0.6
b
b/a
c/a
Orbiting Mass
0.3
0.2
0.1
0
c
Eccentricity
0.6
0.4
0.2
0
d
0
5×10^5
10^6
1.5×10^6
2×10^6
Timesteps (50 sec)